Shock formation in supersonic cluster jets and its effect on axially modulated laser-produced plasma waveguides

S. J. Yoon, A. J. Goers, G. A. Hine, J. D. Magill, J. A. Elle, Y.-H. Chen, and H. M. Milchberg*

Institute for Research in Electronics and Applied Physics, University of Maryland, College Park, MD 20742, USA
**milch@umd.edu*

Abstract: We examine the generation of axially modulated plasmas produced from cluster jets whose supersonic flow is intersected by thin wires. Such plasmas have application to modulated plasma waveguides. By appropriately limiting shock waves from the wires, plasma axial modulation periods can be as small as 70 μm, with plasma structures as narrow as 45 μm. The effect of shocks is eliminated with increased cluster size accompanied by a reduced monomer component of the flow.

OCIS codes: (350.3950) Micro-optics; (350.5400) Plasmas.

References and links

1. H. M. Milchberg, T. R. Clark, C. G. Durfee, T. M. Antonsen, and P. Mora, "Development and applications of a plasma waveguide for intense laser pulses," Phys. Plasmas **3**(5), 2149–2155 (1996).
2. B. D. Layer, A. G. York, T. M. Antonsen, S. Varma, Y.-H. Chen, Y. Leng, and H. M. Milchberg, "Ultrahigh-Intensity Optical Slow-Wave Structure," Phys. Rev. Lett. **99**(3), 035001 (2007).
3. A. G. York, H. M. Milchberg, J. P. Palastro, and T. M. Antonsen, "Direct Acceleration of Electrons in a Corrugated Plasma Waveguide," Phys. Rev. Lett. **100**, 195001 (2008).

S. J. Yoon, J. P. Palastro, D. Gordon, T. M. Antonsen, and H. M. Milchberg, "Quasi-phase-matched acceleration of electrons in a corrugated plasma channel," Phys. Rev. STAB **15**, 081305 (2012).

4. H. Sheng, K. Y. Kim, V. Kumarappan, B. D. Layer, and H. M. Milchberg, "Plasma waveguide efficiently generated by Bessel beams in elongated cluster gas jets," Phys. Rev. E Stat. Nonlin. Soft Matter Phys. **72**, 036411 (2005).

H. M. Milchberg, K. Y. Kim, V. Kumarappan, B. D. Layer, and H. Sheng, "Clustered gases as a medium for efficient plasma waveguide generation," Phil. Trans. R. Soc. A **364**, 647–661 (2006).

5. V. Kumarappan, K. Y. Kim, and H. M. Milchberg, "Guiding of Intense Laser Pulses in Plasma Waveguides Produced from Efficient, Femtosecond End-Pumped Heating of Clustered Gases," Phys. Rev. Lett. **94**(20), 205004 (2005).
6. W. T. Mohamed, G. Chen, J. Kim, G. X. Tao, J. Ahn, and D. E. Kim, "Controlling the length of plasma waveguide up to 5 mm, produced by femtosecond laser pulses in atomic clustered gas," Opt. Express **19**(17), 15919–15928 (2011).
7. B. D. Layer, A. G. York, S. Varma, Y.-H. Chen, and H. M. Milchberg, "Periodic index-modulated plasma waveguide," Opt. Express **17**(6), 4263–4267 (2009).
8. T.-S. Hung, Y.-C. Ho, Y.-L. Chang, S.-J. Wong, H.-H. Chu, J.-Y. Lin, J. Wang, and S.-Y. Chen, "Programmably structured plasma waveguide for development of table-top and photon and particle sources," Phys. Plasmas **19**(6), 063109 (2012).
9. O. F. Hagena and W. Obert, "Cluster Formation in Expanding Supersonic Jets: Effect of Pressure, Temerature, Nozzle Size, and Test Gas," J. Chem. Phys. **56**(5), 1793–1802 (1972).
10. K. Y. Kim, V. Kumarappan, and H. M. Milchberg, "Measurement of the average size and density of clusters in a gas jet," Appl. Phys. Lett. **83**(15), 3210–3212 (2003).
11. Ya. B. Zel'dovich and Yu. P. Raizer, *Physics of Shock Waves and High-Temperature Hydrodynamic Phenomena*, Dover Publications (2002).
12. A. Wada, H. Kanamori, and S. Iwata, "Ab initio MO studies of van der Waals molecule $(N_2)_2$: Potential energy surface and internal motion," J. Chem. Phys. **109**(21), 9434–9438 (1998).
13. H. M. Milchberg, S. J. McNaught, and E. Parra, "Plasma Hydrodynamics of the intense laser-cluster interaction," Phys. Rev. E Stat. Nonlin. Soft Matter Phys. **64**(5), 056402 (2001).
14. T. Ditmire, T. Donnelly, A. M. Rubenchik, R. W. Falcone, and M. D. Perry, "Interaction of intense laser pulses with atomic clusters," Phys. Rev. A **53**(5), 3379–3402 (1996).

#188299 - $15.00 USD Received 4 Apr 2013; revised 10 Jun 2013; accepted 13 Jun 2013; published 25 Jun 2013

15. T. R. Clark and H. M. Milchberg, "Time- and Space-Resolved Density Evolution of the Plasma Waveguide," Phys. Rev. Lett. **78**(12), 2373–2376 (1997).

1. Introduction

Axially-modulated plasma waveguides have been proposed as a means of quasi-phase matching laser plasma interactions for applications including short wavelength generation [1] and direct acceleration of electrons by a high intensity laser pulse [2, 3]. In prior work, we showed that a gas cluster jet is an efficient medium in which to produce laser-generated plasma waveguides [4, 5]. This idea was later pursued by others [6]. We also demonstrated a technique for producing axial modulations in cluster-based plasma waveguides by periodically obstructing the cluster flow using an array of thin wires [7]. This is a simple alternative to demonstrated optical techniques which axially modulate laser intensity at the target [2, 8]. However, in the previous study [7], the axial modulation period was limited to > 200 μm due to the onset of an incompletely understood plasma density drop in the region between the wires.

In this paper, we present a detailed investigation of the origin and mitigation of this density drop by examining jet flow through two wires with variable separation. The density drop is found to be caused by shock waves from supersonic monomer (individual atoms/molecules) dominated gas flow into the wires, which we observe with transverse interferometry and shadowgraphy. As mean cluster size is increased, with an accompanying decrease in monomer concentration, the jet flow becomes more ballistic and the monomer-induced shock amplitude is decreased. By optimizing the cluster jet density and temperature, we have been able to achieve plasma guiding structures with modulation periods as small as70 μm and plasma structures as narrow as 45 μm.

2. Experimental setup

Figure 1 shows the experimental setup. The target is a 15mm by 1mm elongated cluster jet pulsed at 10Hz. To improve cluster formation, the high pressure gas valve was cryogenically cooled to temperatures as low as 93K. Temperature control allows approximate control of the mean cluster size, with larger clusters formed at colder jet temperatures for fixed valve backing pressure. In our experiments, the gas valve was operated to keep the average gas density in the laser interaction zone of the jet constant while varying the mean cluster size. This was accomplished by maintaining the valve backing pressure at 300 psi for temperatures in the range 293 K to 173 K, and 350 psi for 133 K to 93 K. Under these conditions, an increase (decrease) in the cluster size causes a decrease (increase) in the concentration of unclustered atoms/molecules (monomers). The average density in the cluster jet at the peak of the nozzle flow was found by longitudinal interferometry. We found that at 10 Hz jet operation for the range of valve conditions used, the background pressure in our vacuum chamber was proportional to the interferometer-derived density, so we used the background pressure as the proxy for average atom/molecule density in the cluster jet. Monitoring the background pressure allowed straightforward variation of the mean cluster size while keeping the total atom/molecule density at the target approximately constant. The plasma was generated by a 200mJ, 35 fs Ti:Sapphire laser pulse focused at f/25 end-on into the cluster jet. A small portion of the main pulse was split and frequency doubled for use as a transverse interferometric probe pulse. The pump probe time delay was adjustable in the range −1 ns to 3 ns. A sample interferogram and an extracted phase image are shown in Fig. 1. The axially-averaged target neutral gas density profile was measured using an interferometric probe directed through the elongated dimension of the gas jet; the result is in good agreement with plasma density measured at short probe delays with respect to the pump, before appreciable plasma hydrodynamic evolution occurs.

#188299 - $15.00 USD Received 4 Apr 2013; revised 10 Jun 2013; accepted 13 Jun 2013; published 25 Jun 2013

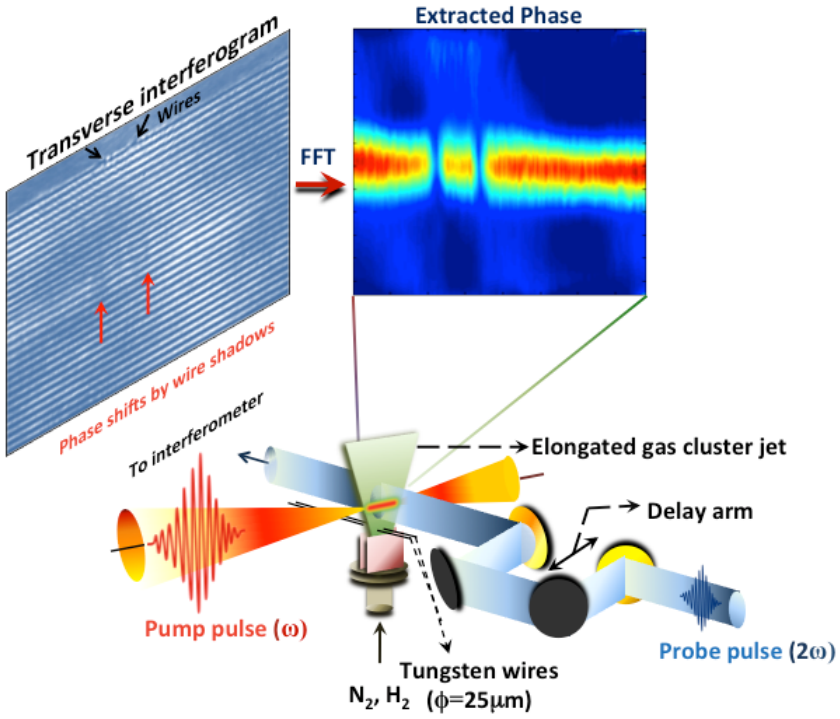

Fig. 1. Experimental setup: Here are shown two 25 μm diameter wires, one mobile and one stationary, placed across the elongated nozzle of a cryogenically cooled supersonic gas jet. A 200mJ, 35fs Ti:Sapphire laser pulse was focused by an f/25 spherical mirror to ionize the cluster target. A portion of the 800nm laser pulse is split from the main beam, frequency doubled, and used as a transverse interferometry/shadowgraphy probe. Shown are an example raw transverse interferogram, followed by results of a Fourier transform analysis yielding the phase shift imposed by the plasma on the probe.

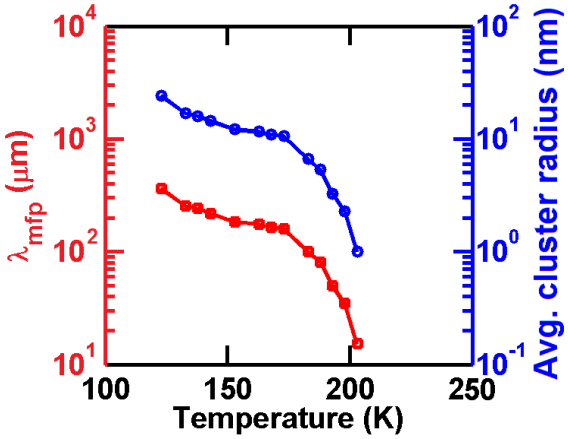

Fig. 2. Average nitrogen cluster size (radius) and collisional mean free path as a function of valve temperature at a backing pressure of 400 psi.

The experiments investigated the effects of one wire, two wires, and an array of wires on the gas flow. Figure 1 shows the case of two parallel 25 μm diameter Tungsten wires strung across in contact with the nozzle exit. One wire remained stationary and the other wire was

#188299 - $15.00 USD Received 4 Apr 2013; revised 10 Jun 2013; accepted 13 Jun 2013; published 25 Jun 2013

attached to an actuator, allowing adjustment of the distance between the wires. The wire separation was measured from phase images of their shadows, as seen in the transverse interferogram in Fig. 1.

3. Analysis of cluster jet flow

The atoms or molecules in a gas flow can bond to form nanometer sized particles called clusters when the mutually induced dipole-dipole attractive potential between particles (van der Waals potential) exceeds in magnitude the particle thermal energy. This can occur in supersonic gas jets when high pressure gas expands rapidly into vacuum and cools.

A well-known semi-empirical relation introduced by Hagena is often used to estimate cluster size for flows from cylindrical nozzles as a function of temperature, valve backing pressure, and nozzle geometry [9]. However, this formula does not apply to our case of an elongated gas jet. To measure average cluster size and number of clusters per unit volume, we developed an all-optical method combining Rayleigh scattering and interferometry [10] and applied it to the elongated jet. The method assumes complete clustering and so is less accurate in the region of higher monomer concentration. However, because the Raleigh scattering part of the measurement strongly favours clusters over monomers, the extracted average cluster size is reasonably accurate, even for significant monomer concentrations up to ~80% [10]. The average cluster radius, for a nitrogen jet backed at 400 psi for a range of valve temperatures, is shown as the blue curve of Fig. 2.

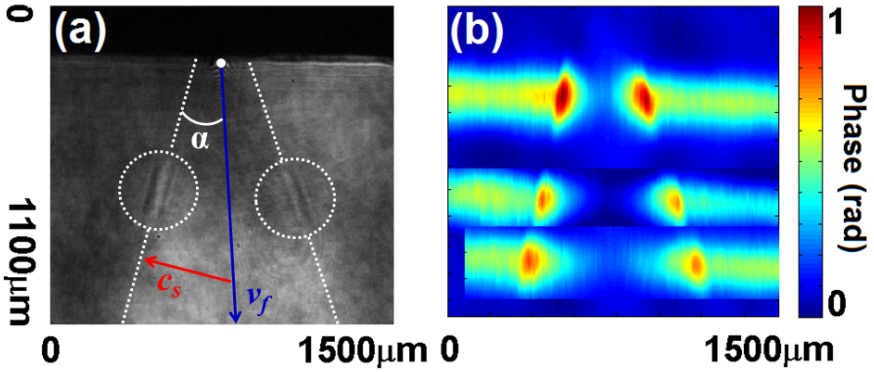

Fig. 3. (a) Shadowgraph of shocks in nitrogen jet flow above a single 25μm tungsten wire, with probe delay 1ps. The wire (indicated by a white dot) is centered on the shocks. The flow is directed down. The valve temperature and pressure were 293K and 300 psi. The blue and red arrows depict the fluid flow and sound velocities, and the dashed white line highlights the shock location. (b) Sequence of extracted phase images of plasma resulting from femtosecond laser interaction with the gas flow 0.5, 0.9 and 1.1mm above the 25μm wire. The laser enters from the left. The probe delay is 1 ps.

The extracted average cluster radius was used to determine a collisional mean free path $\lambda_{mfp} = (N_c\sigma)^{-1}$ for cluster-cluster collisions, where N_c is the density of clusters and σ is the collision cross section. As the inter-cluster potential is very small compared to the cluster kinetic energy, we use $\sigma = \pi a^2$, assuming a hard sphere collision model where a is the average cluster radius. The result is plotted as the red curve of Fig. 2, which shows a quick drop in λ_{mfp} from ~200 μm to < 20 μm as the valve temperature increases from 175K to 200K. Later in the paper, we show that this variation in λ_{mfp} explains the ballistic flow of clusters in the lower temperature gas flow regime and the onset of strong shock waves for higher temperature gas jet flow.

#188299 - $15.00 USD Received 4 Apr 2013; revised 10 Jun 2013; accepted 13 Jun 2013; published 25 Jun 2013

4. One- and two-wire experiments

Initially, we used nitrogen gas with varying valve temperature to observe the effect of cluster size and monomer concentration on the gas flow around the wires. By varying the temperature from 293 K to 93 K, we observed the transition from a normal supersonic gas flow of monomers to the ballistic cluster flow regime. Over this transition, the mean free path of the dominant flow particles goes from much smaller than the spatial scale of any local boundary to much larger. In our case, the local spatial scale is the 25 μm wire diameter. At higher temperatures, the dominant flow particles are monomers, with an interparticle collisional mean free path much smaller than the wire diameter. At lower temperatures, clusters become the dominant flow particle, with infrequent interparticle collisions. The cluster flow is ballistic, and the mean free path is much larger than the wire diameter.

The signature of non-ballistic supersonic gas flow past the wires is generation of shock waves. When an element of collisional fluid collides with the wire, it undergoes local compression. For sub-sonic flows, this pressure disturbance would launch sound waves with a significant component of velocity opposite to the flow direction and with larger magnitude, with some of the waves propagating back to the nozzle orifice. However, for supersonic flow, as is the case here, the pressure disturbance is entrained in the forward fluid flow. The net disturbance propagates as the vector sum of the local sound speed and the supersonic gas flow velocity, giving rise to the refractive index modulations imaged by our interferometric probe beam. Alternatively, and more simply, the wire can be viewed as moving supersonically through a stationary gas, launching angled shock fronts forming a section of a Mach cone. The half-angle of the shock fronts with respect to the flow axis is then given by $\alpha = \sin^{-1}(1/M)$, where $M = v_f/c_s$ is the flow Mach number, c_s is the sound speed, and v_f is the flow speed. Based on the shock angles at different valve temperatures, the Mach number of the flow varies monotonically from $M = 1.2$ at 93K to 1.6 at 293K.

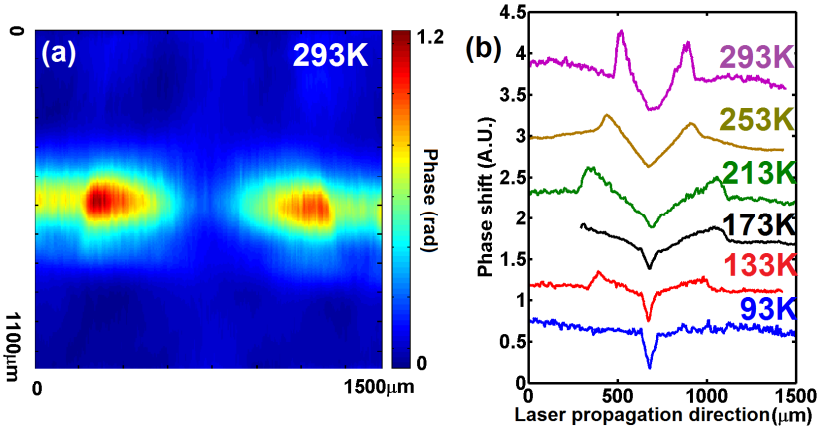

Fig. 4. (a). Phase image of laser-heated plasma produced in nitrogen gas flow at height 1.1 mm above a single 25 μm wire, for probe delay 1 ps. The bumps are increased electron density from laser heating of shock-enhanced gas density zones. (b) Phase lineouts of single wire plasmas (such as in (a)) for a sequence of valve temperatures.

Interaction of the pump pulse with the gas jet with a single wire strung across the nozzle orifice is shown in the shadowgraph in Fig. 3(a), for the case of the valve operated at room temperature (293 K) and 300 psi. Here, as expected for the case of dominant monomer flow, we observe angled shock fronts which manifest as enhanced plasma density at the shock front locations. To aid visualization, the figure shows arrows depicting the gas velocity (blue) and sound velocity (red), a white dot indicating the wire position, and the angle $\alpha = \sin^{-1}(1/M)$. Figure 3(b) is a series of extracted phase images of plasmas generated at 0.5mm, 0.9mm, and 1.1mm above the single wire, where the laser pulse, entering from the left, intersects and

#188299 - $15.00 USD Received 4 Apr 2013; revised 10 Jun 2013; accepted 13 Jun 2013; published 25 Jun 2013

preferentially heats the enhanced density in the increasingly separated local shock fronts, which have a widening region of greatly reduced plasma density between them. The reduced plasma density is evidence that the shocks, which appear to the supersonic flow as a stationary disruptive structure, act to destroy the clusters flowing into them. The entire region of the flow between the shocks is therefore cleared of clusters and the efficiency of the subsequent laser plasma interaction is reduced there.

The destruction of the clusters can be understood by considering the supersonic flow of the partially clustered gas into an oblique shock. Since the shock width is smaller than the other flow scales in the jet, we can approximate the interaction as a flow through a step change in pressure and density subject to conservation of mass, momentum and energy [11]. Under these conditions, the average fluid density (ρ) and pressure (P) upstream and downstream of the shock are related by $\frac{\rho_1}{\rho_2}=\frac{\gamma-1}{\gamma+1}+\frac{2}{(\gamma+1)M^2\sin^2\beta}$ and $\frac{P_2}{P_1}=\frac{2\gamma M^2\sin^2\beta}{\gamma+1}-\frac{\gamma-1}{\gamma+1}$, where "1" refers to upstream and "2" refers to downstream, M is Mach number, β is the flow direction angle with respect to the oblique shock front, and γ = 7/3 is the specific heat ratio for our flow gas, nitrogen, here treated as an ideal gas. The gas temperature change ΔT as a result of flow through the shock front is then given by

$$\frac{T_2}{T_1}=\frac{P_2\rho_1}{P_1\rho_2}=1+\frac{\Delta T}{T}=\left[1+\frac{2\gamma}{\gamma+1}(M^2\sin^2\beta-1)\right]\left[\frac{2+(\gamma-1)M^2\sin^2\beta}{(\gamma+1)M^2\sin^2\beta}\right].$$

Here $\sin\alpha = 1/M$, where α is the angle of the shock from the flow direction at the wire location, and $\beta = \alpha + \delta\alpha$, where $|\delta\alpha/\alpha|<1$. This gives for the gas temperature change,

$$\frac{\Delta T}{T}=4\delta\alpha\left(\frac{\gamma-1}{\gamma+1}\right)\sqrt{M^2-1}.$$

Using γ = 7/3, M in the range 1.2–1.6, and $\delta\alpha/\alpha$~0.3 (from the jet flow geometry) gives $\Delta T/T$ ~0.2–0.3. In the temperature range where there is a significant enough monomer density to form shocks while clusters are still present, there is strong temperature sensitivity of the cluster concentration. Because the van der Waals bond energy for $(N_2)_2$ is ~0.01 eV [12], nitrogen clusters entrained in gas flows at T~150-200K (~0.01–0.02 eV), are vulnerable to decomposition when passing through a shock front where ΔT < ~60K.

Figure 4(a) shows a phase image of nitrogen jet plasma generated over a single 25μm wire for the valve at 293K, where the flow is dominated by monomers. The location of the shock fronts is clearly seen. A central lineout of this image is shown in the top curve of Fig. 4(b), and lineouts of single wire images at decreasing valve temperature are shown as the lower curves. The shockwaves are seen as upward pointing bumps in the phase lineouts. As the temperature is decreased, the shockwave bumps disappear, leaving only the shadow of the wire imposed in the flow, seen as an increasingly fine downward pointing bump. At the higher temperatures, the shock wave from a single wire appears to disrupt the entire flow within its wake, over a transverse extent much larger than the wire diameter.

#188299 - $15.00 USD Received 4 Apr 2013; revised 10 Jun 2013; accepted 13 Jun 2013; published 25 Jun 2013

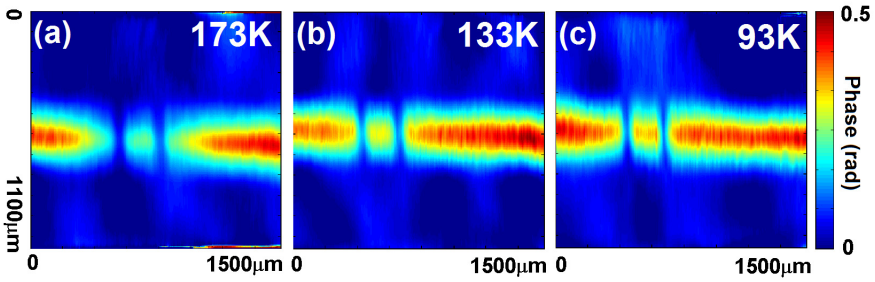

Fig. 5. Phase images, with probe delay 1 ps, of laser heated flow at height 1.1 mm above two wires separated by 150μm at temperature (a) 173K, (b) 133K, and (c) 93K. Increased clustering occurs at reduced temperature.

It is only in the strongly clustered (and ballistic) flow regime at low valve temperatures that a true wire shadow emerges.

The wide shock disruption of the flow past a single wire is the origin, for narrowly spaced wires, of the reduced plasma density from laser heated clusters seen in our earlier experiment [7]. We note from Fig. 4(b) that the shock disruption extends 250 μm on either side of the wire at 133K. This was the valve temperature in the previous study [7], where we found a plasma density drop for wire separations was less than ~200 μm. As discussed earlier, the plasma density drop is caused by shock-induced cluster decomposition, which results in greatly reduced ionization by the laser pulse. Figure 5 shows a sequence of phase plots, for decreasing valve temperature, of plasma generated over two wires separated by 150 μm. Consistent with the results of Fig. 4, it is seen that the sharpest two-wire shadow with the highest in-between density occurs for the lowest valve temperature, 93K, where the shock-generating monomer concentration is the smallest. Only here is the flow sufficiently ballistic that cluster flow between the wires is the same as on either side of the wires.

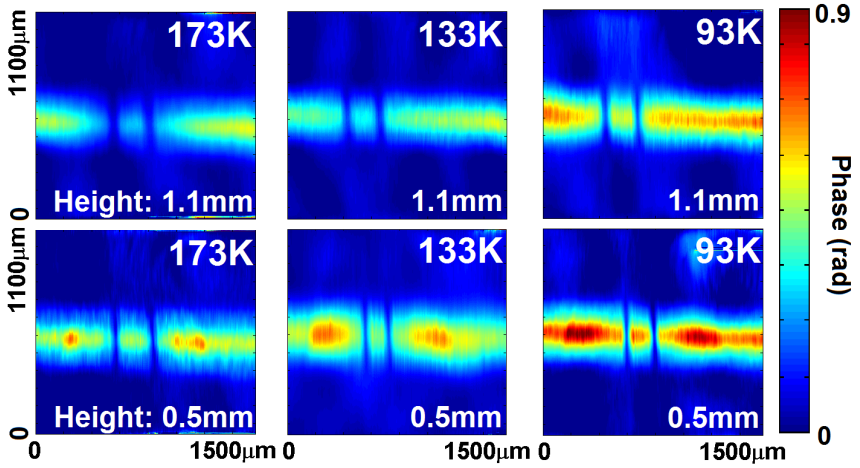

Fig. 6. Phase images of nitrogen plasma generated at heights 0.5 mm and 1 mm above two wire separated by 200 μm, for valve temperatures 133 K, 173 K, and 93 K. The probe delay is 1 ps.

The results of another test for the transition to ballistic cluster flow are shown in the phase images of Fig. 6. Here, plasma was generated at 2 different heights, 0.5 mm and 1.5 mm, above two wires spaced at 200 μm. For highly ballistic flow, one would expect the wire shadows to remain sharp at the higher location with the plasma density maintained between the shadows. This is what is seen for the valve temperature at 93K. As the valve temperature

#188299 - $15.00 USD Received 4 Apr 2013; revised 10 Jun 2013; accepted 13 Jun 2013; published 25 Jun 2013

is increased to 133K and then to 173K, the shadows at the higher location become wider and the plasma density between the shadows drops. From the earlier single wire results, we can attribute the density drop between the shadows to cluster dissociation by shocks launched by each wire into the flow region between the wires. This region widens with height above the wires.

Figure 7 shows extracted phase images of nitrogen plasma with different wire separations for the gas valve at 93K, where we expect ballistic cluster jet flow. This experiment was carried out to determine the minimum wire spacing achievable before the density between the wire shadows begins to drop. This spacing corresponds to the minimum period achievable for a wire-modulated plasma waveguide under our conditions. We found that the density between the wires drops for wire separations less than 70 μm. Below this separation, the wire shadows begin to merge. At 70 μm spacing, the plasma structure width between the wires is ~45 μm.

We now look at how the plasma produced from a wire modulated cluster flow evolves in time. The laser-driven ionization process in a cluster is dominantly collisional, due to its solid density [13, 14]. The heated clusters are strongly ionized and heated and merge into a locally uniform plasma that expands supersonically into the surrounding cluster/gas medium, forming a plasma waveguide structure with a minimum electron density on axis and an elevated outer wall from the outward propagating shockwave [5, 15]. The waveguide generation and evolution is captured with transverse interferometry with varying delay of the probe pulse. The plasma-induced probe phase shift is extracted from the interferogram using fast Fourier transform techniques and the electron density profile is determined by Abel inversion [15], assuming cylindrical symmetry of the plasma channel.

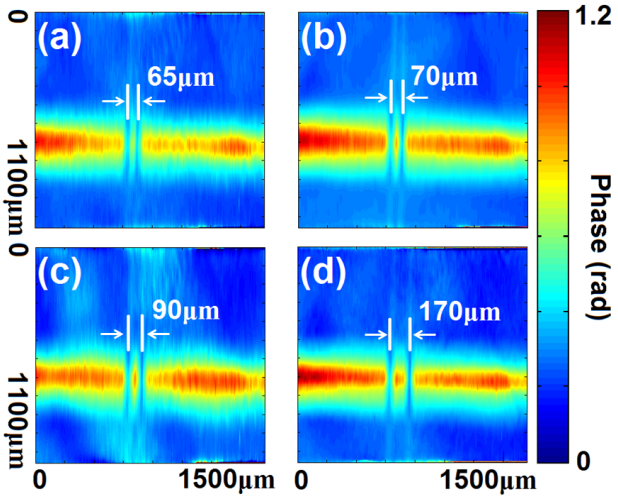

Fig. 7. Phase images of laser produced plasma in a nitrogen cluster jet flowing past two 25μm tungsten wires separated by (a) 65μm, (b) 70μm, (c) 90μm, and (d) 170μm. In each image the gas jet was at 93K and 250PSI backing pressure. The laser propagation is from the left at height 1.1 mm above the wires. The probe delay is 1 ps.

Figure 8 shows the time-evolving electron density profiles for 2-wire experiments with wire spacing 60 μm (part (a)) and 150 μm (part (b)). The delays shown (≥ 0.5 ns) are with respect to plasma generation by the 40 fs pump pulse at $t = 0$. Figure 7 shows the situation for $t = 0$ ns delay, where there is relatively little cluster density in the region between the narrowly spaced (65μm) wire shadows compared to that for the wider (170 μm) spacing. In Fig. 8(a), by 0.5 ns delay the density of the strongly heated plasma between the shadows drops as it expands into the shadow locations. By 1 ns, the in-between density continues to drop and the density at the shadow locations continues to increase, also supplied by high

#188299 - $15.00 USD Received 4 Apr 2013; revised 10 Jun 2013; accepted 13 Jun 2013; published 25 Jun 2013

pressure plasma from outside the shadows. By 2 ns, the plasma begins to fill in the gap between the shadows and by 3 ns, the peak density is located at the shadow gap with an axial scale length of ~60 μm, comparable to the original shadow separation. In Fig. 8(b), as in part (a), the density at first drops in the region between the shadows and increases at the shadow locations. But this trend continues so that by 3 ns, the density is minimum at the in-between region and maximum at the shadow locations. Comparing the evolution shown in Fig. 8(a) and 8(b), we note that the reduced heating of a narrower in-between plasma in (a) means that this region is more susceptible to filling in from adjacent higher pressure plasma regions, so by 3 ns the in-between region hosts a high plasma density. In Fig. 8(b) the denser and more strongly heated in-between region strongly expands outward into the adjacent regions and its density drops. This reduced density is maintained at 3 ns delay.

In Fig. 8, we are also interested in the evolution of the waveguiding structure. For the panels in (a) and (b) for delays >1 ns, a clear on-axis electron density minimum develops, along with a well-defined higher density wall driven by the radially expanding shock wave. Transverse radial lineouts at the location of the vertical dashed lines are shown in Fig. 8(c) (for 8(a)) and Fig. 8(d) (for 8(b)). In both cases, at appropriate delays, the electron density difference between the central minimum of the electron density profile and the shock wall is ~10^{18} cm^{-3} which is sufficient to guide high intensity pulses [1]. This density difference is even greater at other axial locations in the waveguides.

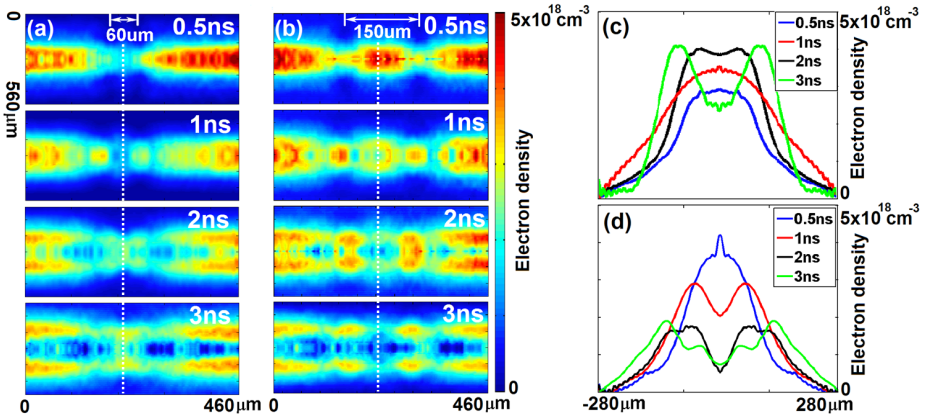

Fig. 8. Electron density profiles of nitrogen plasma channels produced 1.1 mm above the wires, at probe delays: 0.5ns, 1ns, 2ns, and 3ns, with two wire separations: (a) 60 μm and (b)150 μm. (c) Density profile lineouts of (a) along dotted white line. (d) Density profile lineouts of (b) along dotted white line.

5. Experiments with wire arrays

Finally, we fabricated 5-wire arrays of 25μm tungsten wire separated by ~200 μm to produce several periods of axial modulation. Figure 9(a) shows time evolution of a plasma waveguide produced in a nitrogen cluster jet at 93K and 250 psi backing pressure, while Fig. 9(b) is for a 90% hydrogen/10% Ar gas mix cluster jet at 93K and 300psi. In both cases, we expect ballistic cluster flow. It is seen that the hydrogen plasma-based waveguide expands significantly faster than the nitrogen plasma-based guide, owing to the lighter hydrogen ions. It is seen that the sharp wire shadows evident at early pump-probe delays are eventually filled in by the evolving plasma, which expands axially as well as radially.

#188299 - $15.00 USD Received 4 Apr 2013; revised 10 Jun 2013; accepted 13 Jun 2013; published 25 Jun 2013

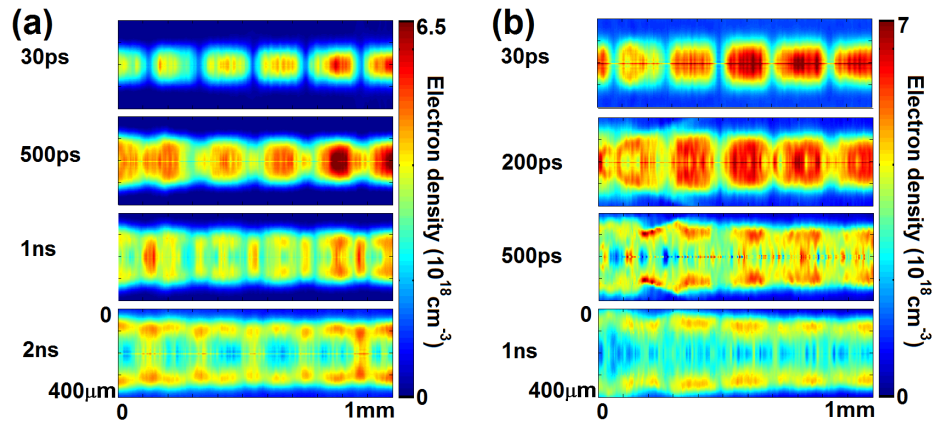

Fig. 9. Time evolution of electron density profiles of plasma waveguides with 200μm axial modulations in (a) a nitrogen cluster jet at 93K and 250 PSI backing pressure and (b) A 90% hydrogen / 10% argon cluster jet backed at 93K and 300 PSI. The waveguides are generated 1.1 mm above the wires.

6. Conclusions

Arrays of wires obstructing gas flow offer a simple and robust method for creating index modulations in plasma waveguides. However, shock waves formed off of the wires act to destroy the clusters that flow into them, reducing the efficiency of subsequent laser heating and a strong reduction in plasma density between the wire shadows. We have shown that increasing the cluster size in the gas jet, which occurs along with a reduction in monomer concentration, transitions the supersonic gas to a ballistic flow regime in which shock effects are negligible and guiding structures with sub-100 μm modulation periods may be achieved.

Acknowledgments

This research is supported by the US Department of Energy, DTRA, the Office of Naval Research, and the National Science Foundation. The authors thank B. D. Layer and K. Y. Kim for useful discussions and technical assistance.

#188299 - $15.00 USD Received 4 Apr 2013; revised 10 Jun 2013; accepted 13 Jun 2013; published 25 Jun 2013